Evaluation of Partial Structure Factors in the Small Q-Region with Amorphous $Ni_{80}P_{20}$ by Neutron Diffraction Using Isotopic Substitution

K. Schild, F. Frisius *, P. Lamparter **, and S. Steeb

Max-Planck-Institut für Metallforschung, Institut für Werkstoffwissenschaften, Seestraße 92, 7000 Stuttgart, Germany

Z. Naturforsch. **40 a,** 551–558 (1985); received March 23, 1985

Amorphous $Ni_{80}P_{20}$-alloys were produced under He-atmosphere by the melt spin technique. With three specimens produced from P with ^{nat}Ni, ^{62}Ni and ^{0}Ni elastic scattering expriments were performed using neutrons with $\lambda = 5.4$ Å in the Q-region $6 \cdot 10^{-3}\,\text{Å}^{-1} \leqq Q \leqq 2.7 \cdot 10^{-1}\,\text{Å}^{-1}$. The measured intensities were corrected for absorption and background, desmeared, and normalized. The partial Bhatia Thornton structure factors S_{NN}, S_{CC}, and S_{NC} were evaluated and allowed the following conclusions: The a-$Ni_{80}P_{20}$-alloy contains regions with radii of about 6.5 Å caused by concentration fluctuations. A method is presented which allows to determine the composition of the regions and the total content of regions within the specimen. In the small Q-region ($6 \cdot 10^{-3}\,\text{Å}^{-1} \leqq Q \leqq 4 \cdot 10^{-2}\,\text{Å}^{-1}$) the run of the partial structure factors is proportional to Q^{-3} caused by concentration- and density-fluctuations. From the partial Fourier transforms follows a slight anisotropy concerning the chemical arrangement with correlation lengths elongated along the ribbon direction.

Introduction

Since the early work [1] on nSAS with a-$Fe_{80}B_{20}$ some further investigations were published, all of them reporting a typical Q^{-3}-behaviour in the very small Q-region with the amorphous alloys $Cu_{78}Tb_{22}$ [2], $Pd_{80}Si_{20}$ [3], $Co_{81.5}B_{18.5}$ [4], and $Pd_{80}(Si_xGe_{1-x})_{20}$ [5]. In [1], using the method of isotopic substitution we discussed the Q^{-3}-behaviour in terms of density fluctuations. Up to now no partial structure factors were reported in the small Q-region. In the present paper we report on such factors which were obtained with the same amorphous $Ni_{80}P_{20}$-alloys used recently for wide angle diffraction experiments [6]. In the latter paper, the partial structure factors were evaluated for $16\,\text{Å}^{-1} \geqq Q \geqq 0.4\,\text{Å}^{-1}$. The present paper continues the Q-region down to $6 \cdot 10^{-3}\,\text{Å}^{-1}$.

Theoretical Fundamentals

1. *Partial structure factors*

Using the Bhatia Thornton formalism [7] the structure of a binary system is described in terms of correlations between density fluctuations and concentration fluctuations, the Fourier transforms of them in Q-space being the partial Bhatia Thornton structure factors $S_{NN}(Q)$, $S_{CC}(Q)$, and $S_{NC}(Q)$. The total structure factor is defined as

$$S^{BT}(Q) = \frac{1}{\langle b^2\rangle}\frac{d\sigma}{d\Omega}(Q), \tag{1}$$

which in terms of the partial structure factors is

$$S^{BT}(Q) = \frac{\langle b\rangle^2}{\langle b^2\rangle} S_{NN}(Q) + \frac{c_A c_B (b_A - b_B)^2}{\langle b^2\rangle} S_{CC}(Q) + \frac{2\langle b\rangle (b_A - b_B)}{\langle b^2\rangle} S_{NC}(Q), \tag{2}$$

where

$S_{NN}(Q)$ = partial structure factor of the correlations between number density fluctuations,
$S_{CC}(Q)$ = partial structure factor of the correlations between concentration fluctuations,
$S_{NC}(Q)$ = partial structure factor of the cross correlations between density fluctuations and concentration fluctuations,
$\frac{d\sigma(Q)}{d\Omega}$ = differential coherent scattering cross section per sterad and atom,
b = scattering length,
$\langle b\rangle = c_A b_A + c_B b_B$,

* GKSS-Forschungs-Zentrum, Geesthacht, Germany
** Metals and Ceramics Division, ORNL, Oak Ridge, Tennessee, USA
Reprint requests to Prof. Dr. S. Steeb, Max-Planck-Institut für Metallforschung, Inst. für Werkstoffwissenschaften, Seestraße 92, D-7000 Stuttgart.

0340-4811 / 85 / 0600-0551 $ 01.30/0. – Please order a reprint rather than making your own copy.

c_A, c_B = atom fractions,
Q = $4\pi(\sin\theta)/\lambda$,
2θ = scattering angle.

To evaluate the three partial functions, three total S^{BT}-functions must be experimentally determined with chemical identical specimens. The scattering length of at least one component must be different for each of the three specimens. In the present case, according to [6] the following selection is convenient:

I) P and ^{nat}Ni, i.e. nickel with natural isotopic abundance,
II) P and ^{62}Ni, i.e. nickel enriched up to 98.5% with the isotope ^{62}Ni,
III) P and ^{0}Ni, i.e. nickel consisting of 26.6% ^{62}Ni and 73.4% ^{60}Ni, so that the resulting scattering length of the Ni-component is zero.

Using these specimens, the following system of three equations is valid for the evaluation of the three partial functions:

$$S(Q)^{I}_{tot} = 0.95\,S_{NN} + 0.05\,S_{CC} + 1.0\,S_{NC}\,, \tag{3}$$

$$S(Q)^{II}_{tot} = 0.53\,S_{NN} + 0.47\,S_{CC} + 2.5\,S_{NC}\,, \tag{4}$$

$$S(Q)^{III}_{tot} = 0.30\,S_{NN} + 0.70\,S_{CC} - 2.3\,S_{NC}\,. \tag{5}$$

The normalized determinant of the weighting coefficients amounts to 0.264 and thus is larger than for a-$Fe_{80}B_{20}$, with which we succeeded to evaluate the partial functions [8].

2. Long wavelength limit

The Bhatia Thornton formalism, originally developed for the description of the molten state can also be applied for the description of the frozen-in state. Thereby the corresponding equations are only valid for the glass-transition temperature T_g. This fact is especially to be observed using the following three equations, which connect the long wavelength limit of the partial structure factors with thermodynamical data:

$$S_{NN}(0) = \varrho_0\,k_B\,T_g\,\varkappa_T + \vartheta^2\,S_{CC}(0)\,, \tag{6}$$

$$S_{CC}(0) = N_A\,k_B\,T_g\,\frac{1}{\left(\frac{\delta^2 G}{\delta c_A^2}\right)_{p,T,N}}\,, \tag{8}$$

$$S_{NC}(0) = -\,\vartheta\,S_{CC}\,, \tag{8}$$

with

$$\vartheta = \varrho_0(V_A - V_B)\,,$$

ϱ_0 = mean atomic density,
k_B = Boltzmann's constant,
$\varkappa_T$ = isothermal compressibility,
N_A = Avogadro's number,
G = free enthalpy of mixing,
V_A, V_B = partial molar volume of species A, B.

For the present case of amorphous $Ni_{80}P_{20}$ the thermodynamical data needed for the evaluation of (6), (7) and (8) are not available. Therefore a preliminary estimation was done according to Miedema's model [9], [10], which, as is well known, contains no statement concerning the distribution of the atoms. Anyhow, this model yields the following figures (see [11]): $S_{NN}(0) \sim 0.01$; $S_{CC}(0) \sim 0.02$; and $S_{NC}(0) \sim -0.01$.

3. Scattering at small Q's

It is not necessary to go into all the details of small angle scattering theory since for the evaluation of the present results we need only the following points:

i) Neutron "small angle scattering" which stands for "Scattering at small Q-values" only occurs if the corresponding specimen contains within a certain matrix (M) regions (R) which differ in their coherent scattering length density $(b\varrho)_R$ from that of the matrix $(b\varrho)_M$. Whether this difference

$$\Delta(b\varrho) = (b\varrho)_R - (b\varrho)_M \tag{9}$$

is based on a difference in the number densities,

$$\Delta(b\varrho) = b\,\Delta\varrho\,, \tag{10}$$

or in the scattering lengths,

$$\Delta(b\varrho) = \varrho_0\,\Delta b\,, \tag{11}$$

is a question which will be answered below for amorphous $Ni_{80}P_{20}$. In the case of (10) the function $S_{NN}(Q)$, and in the case of (11) the function $S_{CC}(Q)$ will show a rise towards smaller Q.

ii) By plotting $\log S(Q)$ vs. $\log Q$ in some cases straight lines observed with different slopes. In the present case this slope is -3 as was already reported for other amorphous alloys in the introduction. Such a run can according to [12] be interpreted as caused by scattering with quasi-dislocations.

iii) By plotting $\ln S(Q)$ vs. Q^2 a so-called Guinier plot is obtained [13]. If a straight line is observed in this case, from its slope the so-called Guinier radius R_G follows, which yields the radius R_b of ball-

shaped particles by the equation

$$R_b = \sqrt{\tfrac{5}{3}}\, R_G . \tag{12}$$

iv) Starting from the well known Bragg equation

$$\lambda = 2d \sin\theta \tag{13}$$

and assuming d to be the diameter of a scattering region we obtain the relationship

$$Q\, d = 2\pi, \tag{14}$$

which allows to estimate the Q-region in which the scattering caused by the diameter d occurs.

v) To obtain the autocorrelation function of particles within the corresponding specimen, the partial structure factors S_{ij} were Fourier-transformed according to:

$$\gamma_{ij}(R) = \int_0^\infty S_{ij}\, Q \sin QR \, \mathrm{d}Q \tag{15}$$

with $\gamma_{ij}(R)$ = partial correlation function of the scattering length density fluctuations.

vi) Quantitative evaluation using the long wavelength limit of the small angle scattering intensity.

The specimen consists of c_R atomic percent regions and c_M atomic percent matrix. Each region consists of c_{NiR} atomic percent Ni and c_{PR} atomic percent phosphorus. During the present section we will present a method which finally yields a relationship between c_{NiR} and c_R (see (36)).

The model calculation starts from the run of S_{CC}, S_{NN}, and S_{NC} as presented in Fig. 1, especially from the region $0.14\ \text{Å}^{-1} \leqq Q \leqq 0.26\ \text{Å}^{-1}$ in which S_{NN} = const, S_{NC} = zero, and S_{CC} increases towards smaller Q-values.

This means the existence of regions with diameters determined from a corresponding Guinier plot to be about 13 Å. The regions all have the same density as the surrounding matrix (S_{NN} = const!) but they have another composition (S_{CC} varying with Q). This means that the SAS in this Q-range mainly is caused by (11).

In a former paper [14] we presented an evaluation method for small angle scattering within the molten state. The present model is to be regarded as more comprehensive since we allow both components, A and B, to exist within the regions at the same time but with different concentrations.

For S_{CC} in Fig. 1 which was obtained from three independent scattering experiments we can state that it is a function which is independent of the radiation with it was obtained. Thus, we arrive using (1) and (2) at a fictive measured coherently scattering cross section per sterad and atom $\frac{\mathrm{d}\sigma}{\mathrm{d}\Omega}(Q)$ if we assume for a thought experiment $\langle b \rangle$ to be zero, i.e.

$$b_A = -\frac{c_B}{c_A} b_B . \tag{16}$$

This procedure is furthermore justified since we will recognize in the final eqn. (36) that the result is independent from any special choice of the scattering lengths at all.

For the special alloy $Ni_{80}P_{20}$ we obtain

$$b_{Ni} = -\,0.25\, b_P . \tag{17}$$

The scattering cross section according to (1) for the case of $Ni_{80}P_{20}$ is given by

$$S_{CC}(Q) = \frac{\frac{\mathrm{d}\sigma}{\mathrm{d}\Omega}(Q)}{0.25\, b_P^2} . \tag{18}$$

This equation is of course also valid for $Q = 0$. The meaning of $\frac{\mathrm{d}\sigma}{\mathrm{d}\Omega}(Q)$ can be evaluated from the common scattering equation of [14], [15]:

$$\frac{\mathrm{d}\sigma}{\mathrm{d}\Omega}(Q) = \frac{w_R\, w_M}{\varrho_0} (b_R\, \varrho_R - b_M\, \varrho_M)^2 \cdot \int_0^\infty 4\pi r^2\, \gamma_0(r) \frac{\sin Qr}{Qr} \mathrm{d}r \tag{19}$$

with

$\frac{\mathrm{d}\sigma}{\mathrm{d}\Omega}(Q)$ = scattering cross section per atom in $10^{-24}\ \text{cm}^2$,
w_R, w_M = volume fraction of the regions or the matrix, respectively,
ϱ_0 = mean atomic density [Å^{-3}],
b_R, b_M = scattering length of the regions or the matrix, respectively [10^{-12} cm],
ϱ_R, ϱ_M = local atomic density within the regions or the matrix, respectively [Å^{-3}],
r = distance [Å],
$\gamma_0(r)$ = normalized autocorrelation function of the scattering length density fluctuations.

For $Q \to 0$, from (19) follows

$$\frac{\mathrm{d}\sigma}{\mathrm{d}\Omega}(0) = \frac{w_R\, w_M}{\varrho_0} (b_R\, \varrho_R - b_M\, \varrho_M)^2\, V_c \tag{20}$$

with

$$V_c = \text{"correlation volume"} = \int_0^\infty 4\pi r^2 \gamma_0(r)\, dr. \quad (21)$$

Comparing (20) with the corresponding equations in [15], [16] we recognize that V_c in those papers was called "volume of one region".

So far it is possible to calculate $\frac{d\sigma}{d\Omega}(0)$ from $S_{CC}(0)$ via (18) and furtheron the difference of scattering length density $\Delta(b\varrho)$ via (20) if only V_c would be known. For the molten state it is always allowed to assume ball shaped regions and thus it is possible to calculate V_c from the radius of gyration. In the present case of amorphous solids, however, V_c must be obtained from integral properties of the scattered intensity. This leads to (compare [16])

$$V_c = \frac{2\pi^2 \frac{d\sigma}{d\Omega}(0)}{\int_0^\infty Q^2 \frac{d\sigma}{d\Omega}(Q)\, dQ}. \quad (22)$$

Equations (20) and (22) yield

$$\int_0^\infty Q^2 \frac{d\sigma}{d\Omega}(Q)\, dQ = \frac{2\pi^2}{\varrho_0} w_R w_M (b_R \varrho_R - b_M \varrho_M)^2. \quad (23)$$

Applying this equation to the 13 Å diameter regions, we use the fact that in Fig. 1 the function S_{NN} is constant, and we therefore postulate

$$\varrho_R = \varrho_M = \varrho_0 = \text{mean atomic number density}. \quad (24)$$

This means in terms of the macroscopic densities D_R and D_M as well as the mean atomic weights $\langle A\rangle_R$ and $\langle A\rangle_M$:

$$\frac{D_R}{\langle A\rangle_R} = \frac{D_M}{\langle A\rangle_M}. \quad (25)$$

For the mathematical treatment of (23), atom fractions are more convenient than volume fractions. Therefore we introduce the Ni- and P-atom fractions c_{NiR} and c_{PR} within the regions as well as the Ni- and P-atom fractions c_{NiM} and c_{PM} within the matrix. Then the following equations hold:

$$c_{NiR} + c_{PR} = c_R, \quad (26)$$

$$c_{NiM} + c_{PM} = c_M, \quad (27)$$

$$c_R + c_M = 1, \quad (28)$$

$$c_{NiR} + c_{NiM} = c_{Ni}, \quad (29)$$

$$c_{PR} + c_{PM} = c_P, \quad (30)$$

$$c_{Ni} + c_P = 1. \quad (31)$$

The relations between the volume fractions w_R and w_M and the atom fractions c_R and c_M, using the condition (25), are:

$$w_R = c_R, \quad (32)$$

$$w_M = c_M. \quad (33)$$

For b_R and b_M from (23), using (17), we write

$$b_R = \frac{c_{NiR} b_{Ni} + c_{PR} b_P}{c_R} = \frac{b_P}{c_R}\left(c_{PR} - \frac{c_{NiR}}{4}\right), \quad (34)$$

$$b_M = \frac{c_{NiM} b_{Ni} + c_{PM} b_P}{c_M} = \frac{b_P}{c_M}\left(c_{PM} - \frac{c_{NiM}}{4}\right). \quad (35)$$

Equations (18, 23–35) finally yield (36), which represents a relationship between c_{NiR} and c_R:

$$\int_0^\infty Q^2 S_{CC}(Q)\, dQ = \frac{2\pi^2 \varrho_0}{c_{Ni} c_P} c_R (1 - c_R)(c_{NiR} - c_R c_{Ni})^2. \quad (36)$$

Equations (36) is independent from the scattering lengths. The value of the integral proves to be $5.14 \cdot 10^{-3}$ Å^{-3}.

The graphical presentation of eqn. (36) will be given below.

Experimental

Nickel with natural isotopic abundance (99.0%, Fa. Ventron) and the Ni-isotopes ^{60}Ni and ^{62}Ni (99.93%, Fa. A. Hempel) as well as phosphorus (99.999%, Fa. Ventron) were alloyed within a closed quartz crucible and then melt spun in He-atmosphere onto a very well polished copper disc. The ribbon thickness was 20 µm, the ribbon width about 1 mm. The ribbons were checked by wide angle X-ray diffraction for the absence of crystalline peaks, and their concentration was determined by an electron microprobe. The macroscopic density was determined using the Archimedian principle in dibromethane as 8.16 g/cm^3 corresponding to a mean atomic density of $\varrho_0 = 0.09$ Å^{-3}. The ribbons were wound around rectangular Al-frames in such a way that the ribbons hit by the beam (about 1×1 cm^2) had all the same orientation.

The measurements were done at the small angle scattering equipment at the beamtube 7 of the reactor FRG 1 of the GKSS research centre.

Two cross-wise mounted position sensitive neutron detectors were used which allowed to detect anisotropic effects produced by the melt spinning process. Two different distances of the sample to the detection plane were used, one with 6.5 meters and one with 1 meter.

The wavelength λ of the neutrons used was about 5.4 Å thus yielding $0.006\,\text{Å} \leqq Q \leqq 0.27\,\text{Å}^{-1}$. Using this wavelength the first peak of the intensity curve does not occur within the angle range of $0 \leqq 2\theta \leqq 180°$ thus avoiding the occurrence of double- and multiple scattering. For performing the evaluation it was necessary to measure the scattering without specimen, the background scattering, the Vanadium scattering etc.

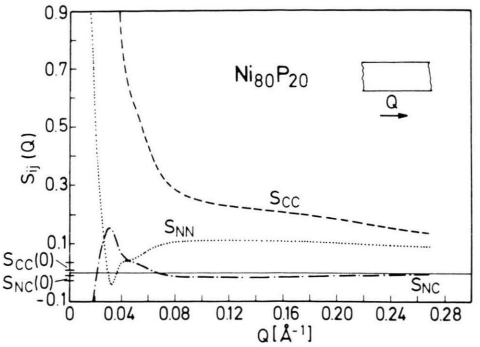

Fig. 1 a. Amorphous $Ni_{80}P_{20}$: Partial structure factors $S_{NN}(Q)$, $S_{CC}(Q)$ and $S_{NC}(Q)$ vs. Q (Q parallel to the ribbon length).

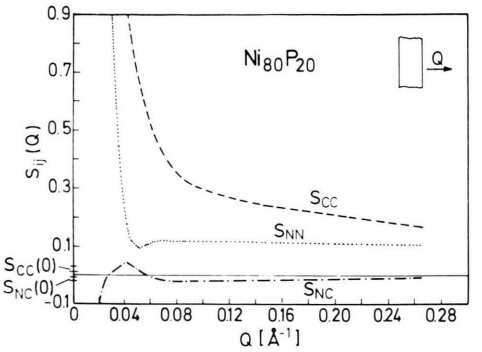

Fig. 1 b. Amorphous $Ni_{80}P_{20}$: Partial structure factors $S_{NN}(Q)$, $S_{CC}(Q)$ and $S_{NC}(Q)$ vs. Q (Q perpendicular to the ribbon length).

Results and Discussion

i) Partial structure factors

Figures 1 a and 1 b show the partial Bhatia Thornton structure factors as obtained parallel and perpendicular to the ribbon length. Starting with Fig. 1 a one can recognize rather different runs of the three partials. S_{NC} is nearly zero along the whole Q-region under observation.

The partial S_{CC} structure factor shows two regions with different gradients. As will be shown later, the run between $0.16\,\text{Å}^{-1}$ and $0.27\,\text{Å}^{-1}$ corresponds to particle diameters of 13 Å. Since in this Q-region S_{NN} remains constant one can conclude that these regions are caused by concentration fluctuations merely. This means that the concentration ratio c_{NiR}/c_{PR} within the regions has another value than within the matrix but that the mean density within the whole sample remains constant.

Within $0.03\,\text{Å}^{-1} \leqq Q \leqq 0.05\,\text{Å}^{-1}$ the run of S_{CC} and S_{NN} in Fig. 1 b is nearly parallel thus indicating regions which are caused as well by concentration-fluctuations as by density-fluctuations and whose auto-correlation function will be determined later.

In Fig. 1 also the values of $S_{CC}(0)$, $S_{NN}(0)$, and $S_{NC}(0)$ as determined according to (6) to (8) are shown. In discussing these values one should keep in mind that they are not based on experimental data but on model calculations, as shown before, and on the other hand that the SAS-data obtained with very small Q's may be influenced for example also by surface scattering effects.

Concerning an anisotropic structure eventually existing within the specimens we can state the following: The three partial functions in Fig. 1 a and Fig. 1 b show nearly the same run, thus indicating isotropic behaviour with one exception, namely the start of the steep rise of $S_{NN}(Q)$ which lies at $0.02\,\text{Å}^{-1}$ and at $0.04\,\text{Å}^{-1}$ in Fig. 1 a and Fig. 1 b, respectively. Since, however, the corresponding Guinier plots of the two S_{NN}-functions show no straight lines in this Q-regions, no evidence can be drawn corresponding to anisotropy effects. This will be done in the following point iv) in which we discuss the run of the corresponding Fourier transforms $\gamma_{NN\perp}$ and $\gamma_{NN\parallel}$.

The smaller regions show an isotropic behaviour for S_{CC} and S_{NN} as well. With increasing Q both functions continuously change over to those obtained with the wide angle scattering experiments [6] which proved a rather strong compound forming tendency.

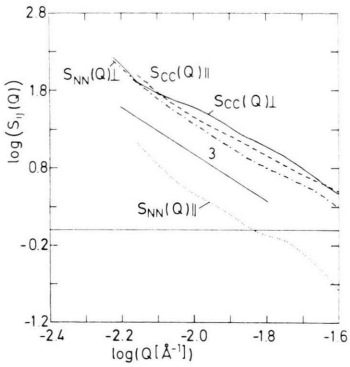

Fig. 2. Amorphous $Ni_{80}P_{20}$: $\log S_{NN}(Q)$ and $\log S_{CC}(Q)$ vs. $\log Q$ in the smallest Q-region (Q parallel or perpendicular, respectively, to the ribbon length).

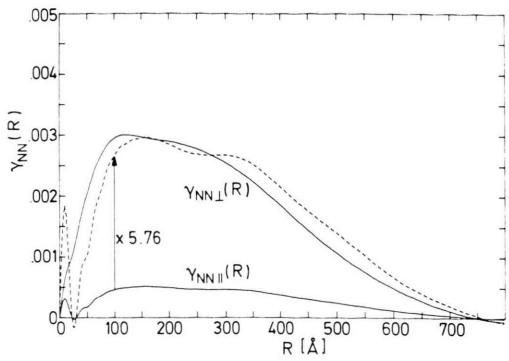

Fig. 4a. Amorphous $Ni_{80}P_{20}$: Partial correlation functions $\gamma_{NN\perp}(R)$ and $\gamma_{NN\parallel}(R)$. Dashed line: Run of $\gamma_{NN\parallel}(R)$ enlarged 5.76 times.

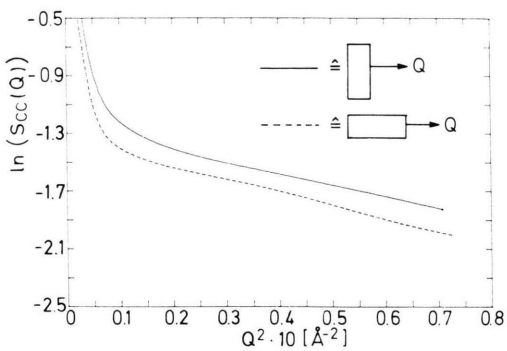

Fig. 3. Amorphous $Ni_{80}P_{20}$: Partial structure factors $\ln S_{CC}(Q)$ vs. Q^2 (Q parallel and perpendicular, respectively, to the ribbon length).

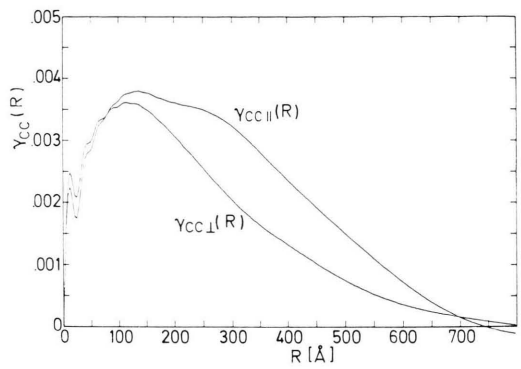

Fig. 4b. Amorphous $Ni_{80}P_{20}$: Partial correlation functions $\gamma_{CC\perp}(R)$ and $\gamma_{CC\parallel}(R)$.

ii) Figure 2 shows the $\log S_{CC}$ vs. $\log Q$ and the $\log S_{NN}$ vs. $\log Q$ plots within the smallest Q-region under observation together with a straight line representing the slope -3. Thus for $Q < 0.03$ Å^{-1} the same behaviour of S_{CC} and S_{NN} in perpendicular ($\perp$) and parallel ($\parallel$) direction as well is obtained, in accordance with the results of other investigations already mentioned in the introduction.

iii) Figure 3 shows the Guinier plot $\ln S_{CC}$ vs. Q^2, which shows a linear run for $0.14\,\text{Å}^{-1} \leqq Q \leqq 0.27\,\text{Å}^{-1}$. This run corresponds to a radius of gyration $R_G = 6.5$ Å.

iv) Figures 4a and 4b show the Fourier transforms $\gamma_{ij}(R)$ vs. R calculated according to (15) from the partial structure factors of Fig. 1a and 1b in the Q-range up to 0.27 Å^{-1}. $\gamma_{ij}(R)$ represents the spectrum of the corresponding correlation lengths.

From Fig. 4a follows, especially when we regard the enlarged run of $\gamma_{NN\parallel}(R)$ (dashed line) a slight shift to larger correlation lengths proceeding from $\gamma_{NN\perp}$ to $\gamma_{NN\parallel}$. Anyhow, the correlation strength, i.e. the ordinate in Fig. 4a is more pronounced along the direction perpendicular to the ribbon direction. Regarding Fig. 4b we recognize that the center of gravity of the $\gamma_{CC\parallel}(R)$-curve is more shifted to larger R-values than $\gamma_{NN}(R)$.

v) Surface scattering occurs from scretches on the surface or surface roughness, which can from the point of view of small angle scattering also be interpreted as vacuum inclusions. Thus it becomes obvious that S_{NN} and S_{CC} caused from surface scattering must be identical. As Fig. 2 shows, this seems to be not the case for the present investigation since $S_{NN\parallel}$ is clearly separated from $S_{NN\perp}$, $S_{CC\perp}$, and $S_{CC\parallel}$.

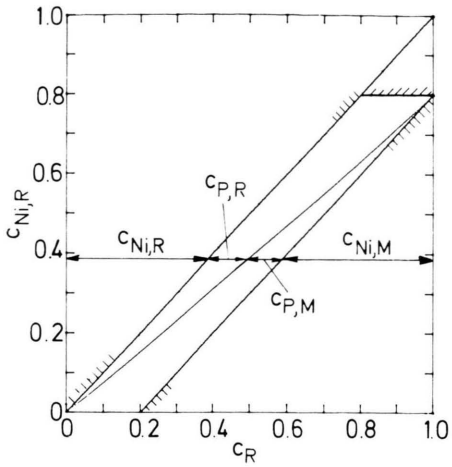

Fig. 5. Amorphous $Ni_{80}P_{20}$: Atom fraction c_{NiR} vs. the atom fraction of regions c_R.

vi) *Quantitative interpretation of the small regions with 13 Å diameter*

From Fig. 1 we learn that the small regions which were in a former paper [1] ascribed to the regions predicted by a computer experiment of Egami et al. [17] have quite another origin. This is because in [17] the small regions are distinguished from their surroundings by internal short range stress which is connected with short range density variations. Figure 1 shows clearly, however, that at least for amorphous $Ni_{80}P_{20}$ these regions are caused exclusively by concentration fluctuations. On the other hand, however, it must be noted that the calculations in [17] were carried out for monatomic systems and thus concentration fluctuations were not to be discussed.

The evaluation of the quantitative method presented in section "Theoretical Fundamentals" yielded Figure 5. It should be mentioned that the calculation yields two similar curves (see [11]) which, however, are symmetrical concerning matrix and regions. Thus it is sufficient to discuss only the one curve presented in Figure 5.

The diagonal area enclosed by the three hatched regions shows up those $c_{NiR}(c_R)$ values which are "allowed" from physical reasons described by (21) to (36). Always on horizontal lines one can pick up the concentrations c_{NiR}, c_{PR}, c_{NiM}, and c_{PM} belonging to a certain c_R as shown as an example for $c_R = 0.50$.

It must be noted as pointed out above that by small angle scattering experiments it is only possible to evaluate the curve presented in Fig. 5 which represents all possible combinations of cencentrations which satisfy (20).

Searching for arguments to discuss one special example led us to the fact that apparently the first product during the crystallization of a-$Ni_{80}P_{20}$ is $Ni_{75}P_{25}$ (see [18], [19]).

The ratio of the nickel and phosphorous concentrations within the very small regions of $c_{NiR}/c_{PR} = 3$ thus seems to be a good choice. The numerical calculation yields the following figures: The whole specimen contains $c_R = 43.8$ a/o regions with the composition $c_{NiR} = 32.85$ a/o and $c_{PR} = 10.95$ a/o i.e. $c_{NiR}/c_{PR} = 3$ within a matrix containing $c_{NiM} = 47.15$ a/o and $c_{PM} = 9.05$ a/o i.e. $c_{NiM}/c_{PM} = 5.21$.

Regarding the overall concentration ratio of the specimen, namely $c_{Ni}/c_P = 4$ it follows that 43.8 a/o of the whole specimen contains a lower nickel-content than the average value and that the surrounding matrix shows up a higher nickel-content than the average.

As is obvious the consideration using $Ni_{75}P_{25}$ regions is only an example and of course may not be regarded as a proof that the regions really existing within the investigated specimens are a preformed alloy $Ni_{75}P_{25}$.

At present we see as one possibility to determine the real, i.e. true combination of concentrations in Fig. 5 an ion probe experiment. As was shown by Piller et al. [20] with a-$Fe_{40}Ni_{40}B_{20}$, it is possible to determine the concentration ratio within regions enriched in one component. Up to now, however, this method was not yet applied to a-$Ni_{80}P_{20}$.

Acknowledgements

Thanks are due to GKSS research centre, Geesthacht, for allocation of beam time and to DFG, Bad Godesberg for financial support.

[1] E. Nold, S. Steeb, and P. Lamparter, Z. Naturforsch. **35 a,** 610 (1980).
[2] B. Boucher, P. Chieux, P. Convert, and M. Tournarie, J. Phys. F **13,** 1339 (1983).
[3] A. Chamberod, B. Rodmacq, J. F. Sadoc, and A. Naudon, ILL-Ann. Report **160** (1983).
[4] J. M. Dubois, F. Bley, and H. Fujara, ILL-Ann. Report **145** (1983).
[5] A. R. Yavari, J. C. Joud, and M. C. Bellissent-Funel, Phys. Let. **105 A,** 88 (1984).
[6] P. Lamparter and S. Steeb, Proc. **RQ 5** (1985), editors: S. Steeb and H. Warlimont.
[7] A. Bhatia and D. E. Thornton, Phys. Rev. **B 2,** 3004 (1970).
[8] E. Nold, P. Lamparter, H. Olbrich, G. Rainer Harbach, and S. Steeb, Z. Naturforsch. **36 a,** 1032 (1981).
[9] A. K. Nissen and A. R. Miedema, Tables of predicted enthalpies of Formation, Solution and Mixing for Binary metal Systems (Philips Research Laboratories, Eindhoven 1982).
[10] R. Boom, F. R. De Boer, and A. R. Miedema, J. Less Common Metals **46,** 271 (1976).
[11] K. Schild, Thesis work, University of Stuttgart 1985.
[12] H. Atkinson and P. B. Hirsch, Phil. Mag. **3,** 213 (1958).
[13] A. Guinier and G. Fournet, Small Angle Scattering of X-Rays, J. Wiley & Sons Inc., New York 1955.
[14] W. Zaiss and S. Steeb, Phys. Chem. Liq. **6,** 43 (1976).
[15] V. Gerold, Z. angew. Physik **9,** 43 (1957).
[16] O. Glatter and O. Kratky, Small Angle X-Ray Scattering, Academic Press, London 1982.
[17] T. Egami, K. Maeda, and V. Vitek, Phil. Mag. A **41** (6), 883 (1980).
[18] U. Pittermann and S. Ripper, Z. Metallkunde **74,** 783 (1983).
[19] E. Vafaei-Makhsoos, E. L. Thomas, and L. E. Toth, Metall. Trans. **9 A,** 1449 (1978).
[20] J. Piller and P. Haasen, Acta Met. **30,** 1 (1981).